The Journal of Chemical Physics ARTICLE pubs.aip.org/aip/jcp

Fast vs slow physical aging of a glass forming liquid

Cite as: J. Chem. Phys. 159, 084504 (2023); doi: 10.1063/5.0167766
Submitted: 14 July 2023 • Accepted: 9 August 2023 •
Published Online: 28 August 2023

Ranko Richert[1,a)] and Jan P. Gabriel[2]

AFFILIATIONS

[1] School of Molecular Sciences, Arizona State University, Tempe, Arizona 85287, USA
[2] Glass and Time, IMFUFA, Department of Science and Environment, Roskilde University, Roskilde 4000, Denmark

[a)] Author to whom correspondence should be addressed: ranko@asu.edu

ABSTRACT

Using electric fields to initiate the process of physical aging has facilitated measurements of structural recovery dynamics on the time scale of milliseconds. This, however, complicates the interesting comparison with aging processes due to a temperature jump, as these are significantly slower. This study takes a step toward comparing the results of field and temperature perturbations by providing data on field-induced structural recovery of vinyl ethylene carbonate at two different time scales: 1.0 ms at 181 K and 33 s at 169 K, i.e., 4.5 decades apart. It is found that structural recovery is a factor of two slower than structural relaxation in equilibrium, with the latter determined via dielectric relaxation in the limit of linear response. The relation between recovery and relaxation dynamics remains temperature invariant across the present experimental range.

I. INTRODUCTION

Physical aging refers to the process of a material approaching equilibrium or steady state conditions after a change in external parameters such as temperature, pressure, or electric field.[1,2] Measurements aimed at characterizing physical aging are typically performed with glass forming materials as a response to a temperature down-jump from above the glass transition temperature T_g, where the system is in equilibrium, to below T_g, where it takes a considerable time for the material to equilibrate.[3–5] Here, equilibrium refers to the metastable, supercooled liquid state of matter, whereas the true equilibrium state below the melting point may be the crystalline state. Recent technical advances have facilitated defined temperature jumps within a matter of seconds, thus providing access to aging measurements on the time scale of minutes rather than hours, days, or weeks.[6] The application of an external electric field will also induce physical aging, provided that the field magnitude is sufficiently high to drive the system beyond the regime of linear response. This approach to aging has the advantage that applying an electric field can be accomplished within microseconds.[7] It has been demonstrated that this approach leads to aging processes on time scales of milliseconds.[8,9] Therefore, if external variables can be modified sufficiently quickly, physical aging can occur quickly and well above the glass transition.

What distinguishes aging in response to a change in the electric field vs temperature is the rate at which the external parameter can be modified, the quadratic dependence on the field amplitude, and the magnitude of the aging response, which is typically very small even for electric fields near the dielectric breakdown limit of the sample. The following will refer to physical aging in this limit of small external perturbations as structural recovery, where the amplitude of the response is proportional to the magnitude of the perturbation. In this context, an interesting question is whether the dynamics of structural recovery are the same for temperature (T), pressure (p), or field (E^2) induced cases. Existing recovery data do not allow for a direct comparison of T-vs E^2-induced recovery, as the experiments have been conducted at very different time scales and temperatures. In fact, it has not yet been demonstrated that field-induced structural recovery well above and near T_g is comparable.

Vinyl ethylene carbonate is a highly polar molecular glass-former with a dipole moment μ = 4.76 D and no pronounced secondary relaxation peak,[10] which are ideal properties for field-induced aging experiments. The aging dynamics can be monitored in the kHz regime (where dielectric loss resolution is high), even

at T_g = 168 K. We show that, apart from the time constant, structural recovery dynamics are the same at 1 ms and 33 s time scales and somewhat slower than the respective α-relaxation times in equilibrium.

II. EXPERIMENTS

Vinyl ethylene carbonate has been obtained from Sigma-Aldrich (VEC, 4-vinyl-1,3-dioxolan-2-one, 99%) and was used as received. The sample is placed between two spring-loaded titanium electrodes, separated by an annular Kapton spacer of 13 μm thickness that leaves an inner 14 mm diameter area filled with the liquid.[11] This cell with C_{geo} = 105 pF is mounted onto the cold stage of a Leybold RDK 6-320 closed-cycle helium refrigerator, with temperatures maintained by a Lakeshore Mod. 340 temperature controller. All measurements were performed on a single sample that remained supercooled for the duration of all the experiments reported here. Low field (linear response) dielectric relaxation spectra, $\varepsilon^*(\omega) = \varepsilon'(\omega) - i\varepsilon''(\omega)$, were recorded with a Solartron SI-1260 gain/phase analyzer, equipped with a DM-1360 transimpedance amplifier, applying electric fields not exceeding 1.5 kV cm^{-1} (<2 V/13 μm) for frequencies 2×10^{-4} Hz $\leq \nu \leq 1 \times 10^{6}$ Hz.

For the high-field structural recovery experiments in the millisecond regime, the field pattern $E(t) = E_B + E_0 \sin(2\pi\nu_0 t)$ is generated by a Stanford Research Systems Arbitrary Waveform Frequency Generator (DS-345) and amplified by a Trek PZD-350 high-voltage unit. The bias field E_B is applied for $t > 0$, and the peak amplitude E_0 of the sinusoidal component is set to 20% of E_B. Voltage $V(t)$ across and current $I(t)$ through the sample are recorded with a Nicolet Sigma 100 Digital Oscilloscope Workstation using a R = 3 kΩ shunt and averaged over 5000 repetitions. The $V(t)$ and $I(t)$ data are subject to Fourier analysis to determine the high bias field dielectric loss ε''_{hi} for each period, resulting in a $\varepsilon''_{hi}(t)$ trace with time resolution $1/\nu_0$. Details regarding setup and analysis can be found elsewhere.[9,12]

For the measurement of slow recovery at a lower temperature, the dielectric loss at a fixed frequency of ν_0 = 400 Hz was acquired with an Andeen-Hagerling AH-2700 Ultra Precision Capacitance Bridge for a duration of 500 s. The sampling rate was one reading every 4 s for the first 280 s and one every 12 s thereafter to increase resolution regarding ε''. A bias voltage of 100 V is derived from a Keithley 6517 Electrometer and applied at t = 0 to the sample using the "DC BIAS" input of the AH-2700 in high-current mode with series resistance R_s = 1 MΩ. With this series resistance, the time constant with which the bias is established at the sample is $R_s \times \varepsilon_s \times C_{geo}$ = 9 ms and, thus, fast relative to the time resolution of the data acquisition. Note that this method can as well be used for longer aging times, and it is technically much simpler than the above setup designed for ms resolution.

III. RESULTS AND DISCUSSION

The dielectric loss profiles of VEC for temperatures T = 169–181 K are shown in Fig. 1, together with Kohlrausch–Williams–Watts (KWW)[13] or stretched exponential fits

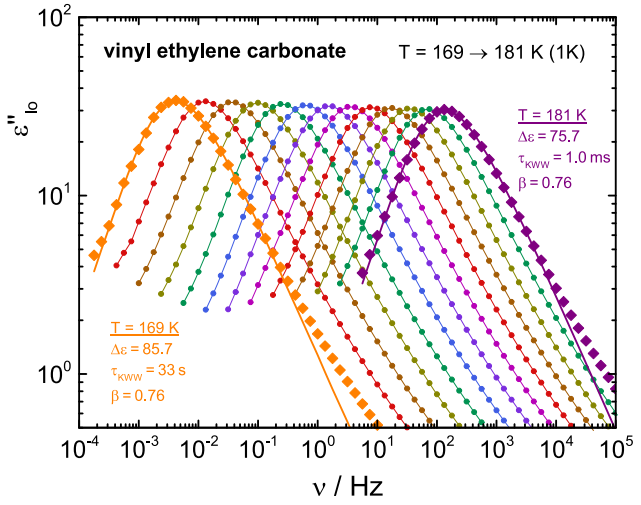

FIG. 1. Low field (linear response) dielectric loss spectra, $\varepsilon''(\nu)$, of vinyl ethylene carbonate for temperatures from 169 to 181 K in steps of 1 K. The KWW fits for the lowest and highest temperatures are shown as solid lines, with the parameters given in the respective legends. Lines for all other temperatures are guides only.

for the highest and lowest temperature based on the Fourier-Laplace transforms of

$$\varepsilon(t) = \varepsilon_\infty + \Delta\varepsilon\left[1 - \exp\left(-\left(\frac{t}{\tau_{KWW}}\right)^{\beta}\right)\right] \quad (1)$$

with the parameters given in the legend in Fig. 1. The shape parameter, β = 0.757, appears to be temperature invariant, consistent with time-temperature superposition within this temperature range, across which τ_{KWW} changes from 33.3 s at 169 K to 1.02 ms at 181 K.

The peak loss frequencies $\nu_{max}(T)$ derived in Fig. 1 have been cast into $\tau_{max} = 1/(2\pi\nu_{max})$ vs temperature, as depicted in Fig. 2, with symbols and colors matching those in Fig. 1. In the present range, the temperature dependence of τ_{max} is well represented by the Vogel–Fulcher–Tammann (VFT) relation,[14–16]

$$\log_{10}(\tau_{max}/\mathrm{s}) = A + \frac{B}{T - T_0} \quad (2)$$

with A = −17.0, B = 695 K, and T_0 = 131.6 K. Apart from a small temperature mismatch, these findings are compatible with previous results on VEC.[10] Regarding the peak time constant, these values yield a glass transition at T_g = 168 K (where τ_{max} = 100 s) and a fragility of m = 87, or strength parameter D = 12, as evaluated directly from the VFT parameters A, B, and T_0.[17] In the present context, an important feature is that τ_{max} changes a factor of 30 000 (4.5 decades) from 168 to 181 K, the two temperatures at which the high-field structural recovery experiments are performed.

The high bias field experiment aims to employ the loss at a fixed frequency ν_0 to monitor how the system approaches the new equilibrium after perturbing it via the application of a high external bias electric field. The net effect of a dc-field is an increase in peak time constant τ_{max},[18–22] leading to a reduction of $\varepsilon''(\nu_0)$, provided that

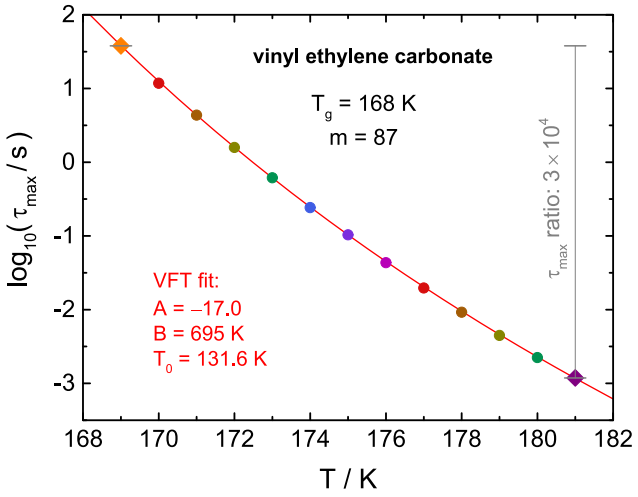

FIG. 2. Temperature dependence of $\tau_{max} = 1/(2\pi\nu_{max})$ for vinyl ethylene carbonate, with the values derived from the peak loss frequencies, ν_{max}, in Fig. 1. The solid line is a VFT fit with the parameters given in the legend. The values of T_g and m are derived from the VFT parameters for $\tau_{max}(T)$. From 169 to 181 K, the value of τ_{max} changes by 3×10^4; see gray bars.

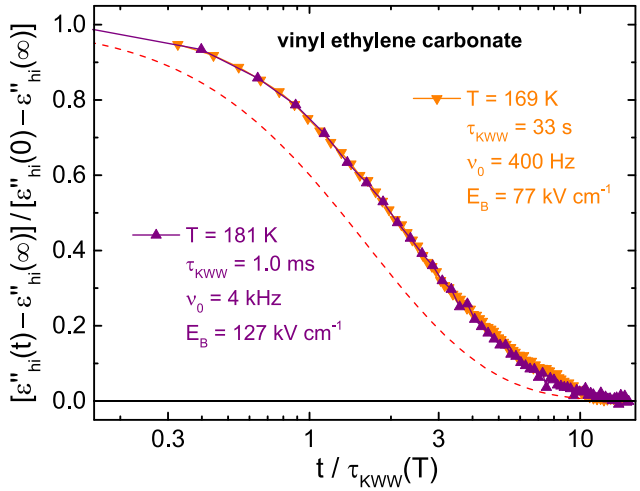

FIG. 3. Time dependent high-field loss, $\varepsilon''_{hi}(t)$, measured at frequency ν_0 and normalized to the value $\varepsilon''_{hi}(0)$ recorded immediately after applying the dc field E_0 and to the long time limit, $\varepsilon''_{hi}(\infty)$. Triangles up and triangles down are for 181 and 169 K, respectively. Solid lines are guides only. The time axis is normalized to the τ_{KWW} value of the corresponding temperature; see the legend. The dashed lines indicate the behavior expected if aging occurred on the time scale of the structural α-relaxation, using Eq. (4a) with $\beta = 0.76$.

$\nu_0 > \nu_{max}$ as in the present experiments. As with temperature induced aging, the change in τ_{max} is not instantaneous but rather follows the slower approach of the fictive field to the actual one.[23] The amplitude of the resulting $\varepsilon''(\nu_0)$ change is a matter of temperature T, frequency ν_0, and bias field amplitude $E_B{}^2$. In order to compare the structural recovery dynamics for T = 168 K, ν_0 = 400 Hz, and E_B = 77 kV cm^{-1} with the one for T = 181 K, ν_0 = 4 kHz, and E_B = 127 kV cm^{-1}, the traces are normalized according to

$$\varepsilon''_{norm}(t) = \frac{\varepsilon''_{hi}(t) - \varepsilon''_{hi}(\infty)}{\varepsilon''_{hi}(0) - \varepsilon''_{hi}(\infty)}, \tag{3}$$

where the subscript "*hi*" refers to the presence of the bias-field E_B. This normalization eliminates the dependence on frequency ν_0 and bias field E_B and yields curves decaying from unity to zero regardless of the actual direction of change. In terms of the $\varepsilon''_{norm}(t)$, the recovery dynamics at the two temperatures are compared in Fig. 3. Because one expects the time scale of structural recovery to change with temperature as the structural relaxation time is derived from a linear response experiment, the time axis in Fig. 3 is normalized to the τ_{KWW} value (see Fig. 1) at the respective temperature.

It is evident from the two experimental datasets in Fig. 3 that the dynamics of field-induced structural recovery are practically identical for the two temperatures, apart from a shift of the recovery time constants τ_{rec} by a factor of 3×10^4 that matches the effect of temperature on τ_{KWW} and τ_{max}. However, this identical temperature effect on τ_{max} and τ_{rec} does not imply that the two time constants are absolutely identical.

In order to facilitate a comparison of τ_{max} and τ_{rec} at a given temperature, the loss peaks in Fig. 1 were fit with a time-domain (KWW, stretched exponential) rather than frequency domain function, so that their dynamics are characterized by the two parameters τ_{KWW} and β. Because the nonlinear dielectric effect in Fig. 3 is quadratic in E_0, the field-induced structural recovery based upon a stretched exponential is expected to follow,[12,23]

$$\varepsilon''^{on}_{norm}(t) \propto \left(1 - \exp\left[-(t/\tau_{KWW})^{\beta}\right]\right)^2 \tag{4a}$$

and

$$\varepsilon''^{off}_{norm}(t) \propto \left(\exp\left[-(t/\tau_{KWW})^{\beta}\right]\right)^2 \tag{4b}$$

for the cases of applying (on) and removing (off) the field, respectively. Using Eq. (4a) and the stretching parameter β = 0.76 for the structural α-relaxation, the dashed line in Fig. 3 shows the structural recovery dynamics that would be expected if identical to the relaxation counterpart derived from linear response dielectric data. Moreover, any field step, up or down, will lead to the sample absorbing energy from the field, which results in a transient rise in the fictive temperature and, thus, a rise in $\varepsilon''(\nu_0)$ for $\nu_0 > \nu_{max}$. Although this "heating" like feature can be modeled quantitatively,[12] it will be demonstrated below that a multi field-step experiment can reduce uncertainties regarding this correction considerably.

Figure 4(a) depicts the bias field pattern used for an experiment to access the dynamics of structural recovery. At time t = 0, a field of magnitude E_B = 138 kV cm^{-1} is applied, followed after 22 ms by another step to E_B = 193 kV cm^{-1}, and E_B drops to 138 kV cm^{-1} again for t > 44 ms. The E_B levels are designed to have two steps of the same magnitude regarding $E_B{}^2$, to which the loss change is proportional. However, the second step height is smaller than the first, leading to nearly negligible energy absorption effects for the transitions from E_B = 138

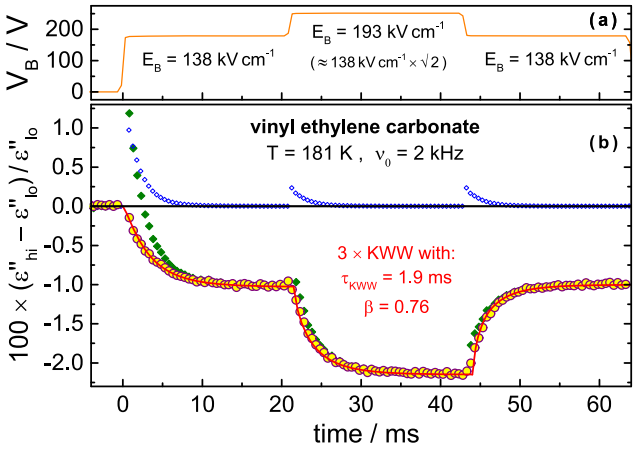

FIG. 4. (a) Voltage bias, V_B, applied to the vinyl ethylene carbonate sample at T = 181 K. (b) Relative dc-field induced change of the dielectric loss, ε''_{hi}, measured at ν_0 = 2 kHz with the applied bias voltage shown in panel (a). Green solid diamonds are for the ε''_{hi} values as observed; blue open diamonds represent the calculated effect of elevated fictive temperatures due to energy absorption from the field; and yellow circles are the "heating" corrected values. The red solid line is the calculated response, assuming that aging progresses according to a stretched exponential with τ_{KWW} = 1.9 ms and β = 0.76.

to 193 kV cm^{-1} and back. The solid green diamonds in Fig. 4(b) show the field-induced relative change of $\varepsilon''(\nu_0)$ as observed. Open blue diamonds represent the calculated "heating" effect, based on a probability density, $g(\tau_D)$, of independent Debye modes with time constant τ_D,[24,25] each absorbing a time-dependent power $p(t)$ according to[12]

$$p(t) = \varepsilon_0 \upsilon E_B^2 \Delta\varepsilon \frac{1}{\tau_D} \exp\left(-\frac{2t}{\tau_D}\right) g(\tau_D) d\tau_D, \tag{5}$$

where ε_0 is the permittivity of the vacuum and υ is the sample volume. The effective temperature change of each mode is determined by the energy absorbed, $p(t)\,dt$, and the heat capacity, $\Delta C_{cfg} \times g(\tau_D) d\tau_D$, where ΔC_{cfg} is the configurational contribution to the glass-to-liquid heat capacity step. Open circles with a yellow interior represent the relative change in ε''_{hi} after correction for the energy absorption effects. For the transitions at 22 and 44 ms, this correction is almost negligible, whereas it is significant for the t = 0 step. The corrected data representing the true structural recovery effect (circles) is modeled by the squared stretched exponentials of Eq. (4), with Eqs. (4a) and (4b) capturing the response to the field up-step and down-step, respectively.

It can be observed in Fig. 4 that the magnitudes of the ε''_{hi} changes are the same for the E_B = 0–138 kV cm^{-1} and E_B = 138–193 kV cm^{-1} transitions, about −1% each. This confirms the expected quadratic field dependence of this nonlinear dielectric effect. The red lines are stretched exponential fits to the response to each field step, and all three curves are calculated with a common parameter set, τ_{KWW} = 1.9 ms and β = 0.76. While accounting for the quadratic field dependence via Eq. (4), a common KWW type time dependence captures the asymmetry of the up vs down transitions. Therefore, field-induced structural recovery in supercooled VEC is a factor of about two slower than linear response structural relaxation in equilibrium with τ_{KWW} = 1.0 ms but reveals the same stretching exponent β. This behavior is maintained across the present temperature interval, 169–181 K, in which τ_{KWW} covers a range from 1.0 ms to 33 s, i.e., a factor of 3 × 10^4.

It should be noted that the common models of physical aging, the Tool–Narayanaswamy–Moynihan (TNM)[26–28] and the equivalent Kovacs–Aklonis–Hutchinson–Ramos (KAHR)[29] approach, assume the identity of structural relaxation (τ_α) and structural recovery (τ_{rec}) dynamics in this limit of very small perturbations. In the present high bias field cases, τ_{max} had increased by about 1.5% relative to its low field limit, which is a small fraction of the difference between recovery and relaxation time constants of 200%. These 1.5% changes regarding τ_{max} are the equivalent of what a 15 mK temperature down-jump would achieve. Based on actual temperature jump induced aging experiments on VEC with ΔT between 10 and 100 mK, the present situation is safely within the limit of small perturbation.[30]

One consequence of τ_{max} changing only 1.5% in the course of the aging process is that changes in material time or fictive temperature remain negligible, and fitting with a constant τ_{rec} instead of using TNM or similar analysis tools is entirely justified. An estimate shows that the difference between accounting for the change in material time and disregarding it will not exceed the width of the dashed line in Fig. 3 and is thus small compared with experimental noise. Therefore, the factor of two separating structural relaxation (τ_α) from structural recovery (τ_{rec}) is robust and not impacted by the present choice of analysis. One may wonder whether τ_{rec} will approach τ_α if the perturbation (field step amplitude) is made smaller. If the electric field is kept significantly smaller than about 100 kV cm^{-1}, there will be no measurable change in τ_α in such a regime of linear response. Consequently, the system would remain in equilibrium, no structural recovery would occur, and τ_{rec} would not be defined. In the comparison of enthalpy relaxation times for large and small temperature excursions ΔT, the time constant would gradually approach the linear limit with $\Delta T \to 0$.[30,31] In the present case, however, τ_α is measured in equilibrium without any change in thermodynamic potential, while τ_{rec} is determined in response to a change in the thermodynamic potential but within the limit of a small change. Therefore, the two time constants refer to distinct processes, and τ_{rec} will not necessarily become τ_α in the limit of small perturbations.

The present finding of the factor of two between τ_{rec} and τ_α is material specific. Other supercooled liquids have been characterized by high-field dielectric experiments regarding their ratio $\rho = \tau_{rec}/\tau_\alpha$, albeit only in the regime of millisecond dynamics. The values reported thus far are ρ = 1.0 for propylene glycol,[32] ρ = 1.4 for glycerol,[8] ρ = 1.5 for cresolphthalein dimethylether,[33] ρ = 2.0 for N-methyl-ε-caprolactam,[22] ρ = 1.9 for the present case of VEC, and ρ = 3.0 for 2-methyltetrahydrofuran.[8] These numbers suggest that structural recovery is linked more closely to the time scale of rate-exchange[24,25] than to structural relaxation,[7,8,34] where rate-exchange refers to the fluctuations of time constants in equilibrium.[35] Moreover, the standard assumption made when modeling physical aging or differential scanning calorimetry, i.e., that the dynamics of structural recovery (τ_{rec}) and structural relaxation in equilibrium (α-process, τ_α) are identical, is not consistent with the observations of $\tau_{rec} > \tau_\alpha$.

IV. SUMMARY AND CONCLUSIONS

Structural recovery dynamics in response to steps in the external electric field have been measured for vinyl ethylene carbonate at two temperatures, $T = 169$ K and $T = 181$ K, at which the respective peak relaxation time constants τ_{max} are 38 s and 1.2 ms, i.e., separated by 4.5 decades. It is found that structural recovery, i.e., physical aging in the limit of small perturbations, is slower than structural relaxation dynamics as derived from linear-response dielectric relaxation spectroscopy. If compared on the basis of stretched exponential behavior, structural recovery follows a KWW type decay of the form $\propto \exp\left[-(t/2\tau_\alpha)^\beta\right]$, where τ_α and β are the KWW parameters describing the structural relaxation in equilibrium. This material specific factor of about two regarding the characteristic time constants remains unchanged across the present temperature range, $T_g + 1$ K to $T_g + 23$ K. This result facilitates a future comparison between field and temperature induced structural recovery. The two processes are not necessarily expected to be identical, as a temperature change leaves the liquid in an isotropic state, whereas external electric fields impose anisotropy on polar liquids.

ACKNOWLEDGMENTS

This research was supported by the National Science Foundation under Grant No. DMR-1904601.

AUTHOR DECLARATIONS

Conflict of Interest

The authors have no conflicts to disclose.

Author Contributions

Ranko Richert: Conceptualization (lead); Formal analysis (equal); Funding acquisition (lead); Investigation (lead); Validation (equal); Writing – review & editing (equal). **Jan P. Gabriel**: Formal analysis (equal); Validation (equal); Writing – review & editing (equal).

DATA AVAILABILITY

The data that support the findings of this study are available from the corresponding author upon reasonable request.

REFERENCES

[1] L. C. E. Struik, "Physical aging in amorphous glassy polymers," Ann. N. Y. Acad. Sci. **279**, 78 (1976).
[2] I. M. Hodge, "Enthalpy relaxation and recovery in amorphous materials," J. Non-Cryst. Solids **169**, 211 (1994).
[3] A. J. Kovacs, "La contraction isotherme du volume des polymères amorphes," J. Polym. Sci. **30**, 131 (1958).
[4] P. Lunkenheimer, R. Wehn, U. Schneider, and A. Loidl, "Glassy aging dynamics," Phys. Rev. Lett. **95**, 055702 (2005).
[5] R. Richert, P. Lunkenheimer, S. Kastner, and A. Loidl, "On the derivation of equilibrium relaxation times from aging experiments," J. Phys. Chem. B **117**, 12689 (2013).
[6] T. Hecksher, N. B. Olsen, K. Niss, and J. C. Dyre, "Physical aging of molecular glasses studied by a device allowing for rapid thermal equilibration," J. Chem. Phys. **133**, 174514 (2010).
[7] R. Richert, J. P. Gabriel, and E. Thoms, "Structural relaxation and recovery: A dielectric approach," J. Phys. Chem. Lett. **12**, 8465 (2021).
[8] B. Riechers and R. Richert, "Rate exchange rather than relaxation controls structural recovery," Phys. Chem. Chem. Phys. **21**, 32 (2019).
[9] R. Richert, "Nonlinear dielectric effects in liquids: A guided tour," J. Phys.: Condens. Matter **29**, 363001 (2017).
[10] A. Jedrzejowska, Z. Wojnarowska, K. Adrjanowicz, K. L. Ngai, and M. Paluch, "Toward a better understanding of dielectric responses of van der Waals liquids: The role of chemical structures," J. Chem. Phys. **146**, 000013 (2017).
[11] K. Adrjanowicz, M. Paluch, and R. Richert, "Formation of new polymorphs and control of crystallization in molecular glass-formers by electric field," Phys. Chem. Chem. Phys. **20**, 925 (2018).
[12] A. R. Young-Gonzales, S. Samanta, and R. Richert, "Dynamics of glass-forming liquids. XIX. Rise and decay of field induced anisotropy in the non-linear regime," J. Chem. Phys. **143**, 104504 (2015).
[13] G. Williams and D. C. Watts, "Non-symmetrical dielectric relaxation behaviour arising from a simple empirical decay function," Trans. Faraday Soc. **66**, 80 (1970).
[14] H. Vogel, "Das Temperaturabhängigkeitsgesetz der Viskosität von Flüssigkeiten," Phys. Z. **22**, 645 (1921).
[15] G. S. Fulcher, "Analysis of recent measurements of the viscosity of glasses," J. Am. Ceram. Soc. **8**, 339 (1925).
[16] G. Tammann and W. Hesse, "Die abhängigkeit der viscosität von der temperatur bie unterkühlten flüssigkeiten," Z. Anorg. Allg. Chem. **156**, 245 (1926).
[17] C. A. Angell, "Relaxation in liquids, polymers and plastic crystals—Strong/fragile patterns and problems," J. Non-Cryst. Solids **13**, 131–133 (1991).
[18] C. T. Moynihan and A. V. Lesikar, "Comparison and analysis of relaxation processes at the glass transition temperature," Ann. N. Y. Acad. Sci. **371**, 151 (1981).
[19] G. P. Johari, "Effects of electric field on the entropy, viscosity, relaxation time, and glass-formation," J. Chem. Phys. **138**, 154503 (2013).
[20] D. L'Hôte, R. Tourbot, F. Ladieu, and P. Gadige, "Control parameter for the glass transition of glycerol evidenced by the static-field-induced nonlinear response," Phys. Rev. B **90**, 104202 (2014).
[21] D. V. Matyushov, "Configurational entropy of polar glass formers and the effect of electric field on glass transition," J. Chem. Phys. **145**, 034504 (2016).
[22] S. Samanta and R. Richert, "Electrorheological source of nonlinear dielectric effects in molecular glass-forming liquids," J. Phys. Chem. B **120**, 7737 (2016).
[23] B. Riechers and R. Richert, "Structural recovery and fictive variables: The fictive electric field," Thermochim. Acta **677**, 54 (2019).
[24] M. D. Ediger, "Spatially heterogeneous dynamics in supercooled liquids," Annu. Rev. Phys. Chem. **51**, 99 (2000).
[25] R. Richert, "Heterogeneous dynamics in liquids: Fluctuations in space and time," J. Phys.: Condens. Matter **14**, R703 (2002).
[26] A. Q. Tool, "Relation between inelastic deformability and thermal expansion of glass in its annealing range," J. Am. Ceram. Soc. **29**, 240 (1946).
[27] O. S. Narayanaswamy, "A model of structural relaxation in glass," J. Am. Ceram. Soc. **54**, 491 (1971).
[28] M. A. DeBolt, A. J. Easteal, P. B. Macedo, and C. T. Moynihan, "Analysis of structural relaxation in glass using rate heating data," J. Am. Ceram. Soc. **59**, 16 (1976).
[29] A. J. Kovacs, J. J. Aklonis, J. M. Hutchinson, and A. R. Ramos, "Isobaric volume and enthalpy recovery of glasses. II. A transparent multiparameter theory," J. Polym. Sci., Polym. Phys. Ed. **17**, 1097 (1979).
[30] B. Riechers, L. A. Roed, S. Mehri, T. S. Ingebrigtsen, T. Hecksher, J. C. Dyre, and K. Niss, "Predicting nonlinear physical aging of glasses from equilibrium relaxation via the material time," Sci. Adv. **8**, eabl9809 (2022).
[31] J. Hadač, P. Slobodian, P. Říha, P. Sáha, R. W. Rychwalski, I. Emri, and J. Kubát, "Effect of cooling rate on enthalpy and volume relaxation of polystyrene," J. Non-Cryst. Solids **353**, 2681 (2007).
[32] R. Richert, "One experiment makes a direct comparison of structural recovery with equilibrium relaxation," J. Chem. Phys. **157**, 224501 (2022).
[33] S. Samanta, O. Yamamuro, and R. Richert, "Connecting thermodynamics and dynamics in a supercooled liquid: Cresolphthalein-dimethylether," Thermochim. Acta **636**, 57 (2016).

[34]S. Samanta and R. Richert, "Limitations of heterogeneous models of liquid dynamics: Very slow rate exchange in the excess wing," J. Chem. Phys. **140**, 054503 (2014).

[35]A. Heuer, M. Wilhelm, H. Zimmermann, and H. W. Spiess, "Rate memory of structural relaxation in glasses and its detection by multidimensional NMR," Phys. Rev. Lett. **75**, 2851 (1995).